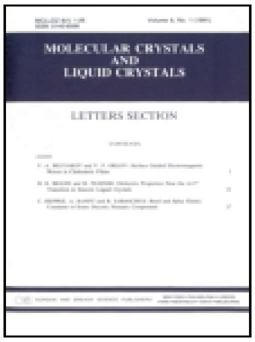

Taylor & Francis
Taylor & Francis Group

Molecular Crystals and Liquid Crystals

ISSN: 1542-1406 (Print) 1563-5287 (Online) Journal homepage: http://www.tandfonline.com/loi/gmcl20

Structure and Characterization of a Novel Chalcone Crystal Having Nitro as an Acceptor Group

Shobha R. Prabhu, A. Jayarama, V. Upadhyaya, K. Subrahmanya Bhat & Seik Weng Ng

To cite this article: Shobha R. Prabhu, A. Jayarama, V. Upadhyaya, K. Subrahmanya Bhat & Seik Weng Ng (2015) Structure and Characterization of a Novel Chalcone Crystal Having Nitro as an Acceptor Group, Molecular Crystals and Liquid Crystals, 607:1, 200-214, DOI: 10.1080/15421406.2014.928434

To link to this article: http://dx.doi.org/10.1080/15421406.2014.928434

Mol. Cryst. Liq. Cryst., Vol. 607: pp. 200–214, 2015
Copyright © Taylor & Francis Group, LLC
ISSN: 1542-1406 print/1563-5287 online
DOI: 10.1080/15421406.2014.928434

Structure and Characterization of a Novel Chalcone Crystal Having Nitro as an Acceptor Group

SHOBHA R. PRABHU,[1,2,*] A. JAYARAMA,[3] V. UPADHYAYA,[2]
K. SUBRAHMANYA BHAT,[4] AND SEIK WENG NG[5,6]

[1]Department of Physics, NMAM Institute of Technology, Nitte, Karnataka, India
[2]Department of Physics, Manipal Institute of Technology, Manipal University, Manipal, India
[3]Department of Physics, Sadguru Swami Nithyananda Institute of Technology (SSNIT), Kanhangad 671315, India
[4]Department of Chemistry, Manipal Institute of Technology, Manipal University, Manipal, India
[5]Department of Chemistry, University of Malaya, Kuala Lumpur, Malaysia
[6]Chemistry Department, Faculty of Science, King Abdulaziz University, Jeddah

*A novel organic nonlinear optical (NLO) compound (2*E*)-3-(2-methylphenyl)-1-(4-nitrophenyl) prop-2-en-1-one (2MPNP) has been synthesized and grown as a high-quality single crystal by the slow evaporation technique. 2MPNP crystals were characterized by FT-IR, UV-Vis-NIR, NMR, DSC, and Single Crystal XRD techniques. 2MPNP crystallizes in the orthorhombic crystal class in the noncentrosymmetric space group $Pca2_1$ with cell parameters $a = 29.905(4)$ Å, $b = 4.8241(5)$ Å, $c = 9.0984(10)$ Å, $\alpha = \beta = \gamma = 90.00°$, and $V = 1312.58$ Å^3 and $Z = 4$. Second harmonic generation (SHG) efficiency of the grown crystal was found to be 1.17 times that of urea. Thermal analysis reveals that the crystal has better thermal stability.*

Keywords: Chalcones; characterization; crystal structure; nonlinear optical materials

Introduction

The development of optical fiber communication systems and photonics requires new highly nonlinear materials capable of fast and efficient processing of optical signals. Organic nonlinear optical (NLO) crystals have proven to be interesting candidates for a certain applications like second-harmonic generation, frequency mixing, electro-optic modulation, optical parametric oscillation, optical switching, and optical data storage [1]. Organic NLO materials possess large second order nonlinearity and offer an opportunity to use theoretical modeling coupled with synthetic flexibility to design and produce newer materials [1, 2]. The basic structural requirement of organic NLO materials is extended π-bond system preferably linked by aromatic groups with strong donor and acceptor end which may lead

---

[*]Address correspondence to Shobha R. Prabhu, Department of Physics, NMAM Institute of Technology, Nitte 574110, Karnataka, India. Tel: +918258 281264, Fax: +918258 281265. E-mail: shobha@nitte.edu.in

Color versions of one or more of the figures in the article can be found online at www.tandfonline.com/gmcl.

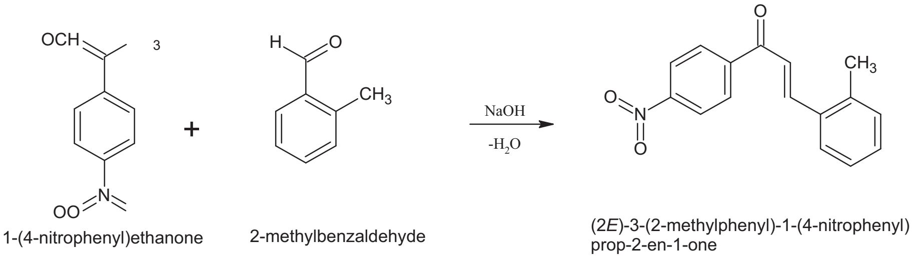

Figure 1. Synthesis scheme of 2MPNP.

to delocalization of electronic charge distribution imparting higher optical nonlinearity. Several structural manipulations can be done by having appropriate donor or acceptor group at ortho, meta, or para positions of aromatic ring [2–5].

The chalcones are α,β-unsaturated ketones containing the keto ethylenic group $-\mathrm{CO}-\mathrm{CH}=\mathrm{CH}-$ that exhibit good second harmonic generation (SHG) efficiency and transparency [6–9]. The NLO behavior of the chalcone molecules originates mainly from a strong donor–acceptor intermolecular interaction and delocalized π-electron system. Several molecules can be synthesized by adopting suitable design strategies, such as donor–π–acceptor (D–π–A), donor–π–donor (D–π–D), donor–acceptor–donor (D–A–D), and acceptor–donor–acceptor (A–D–A) [10, 11]. Recently, we have synthesized and investigated the crystal structure of chalcone with hydroxyl functional group [12, 13]. It is also possible to incorporate heterocyclic ring like thiophene and improve crystallizability of the molecules [14–16].

In this paper, synthesis, growth, structural characterization, and second order NLO property of novel D–π–A type compound (2*E*)-3-(2-methylphenyl)-1-(4-nitrophenyl) prop-2-en-1-one (2MPNP) has been reported.

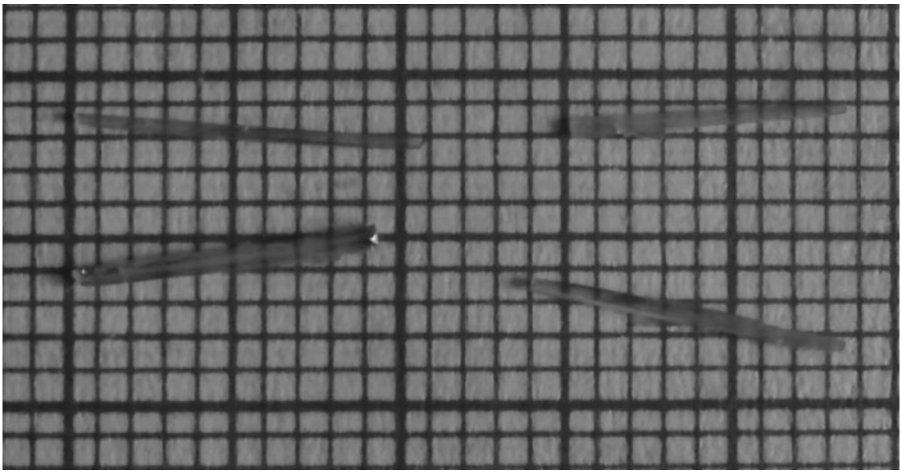

Figure 2. Single crystals of 2MPNP.

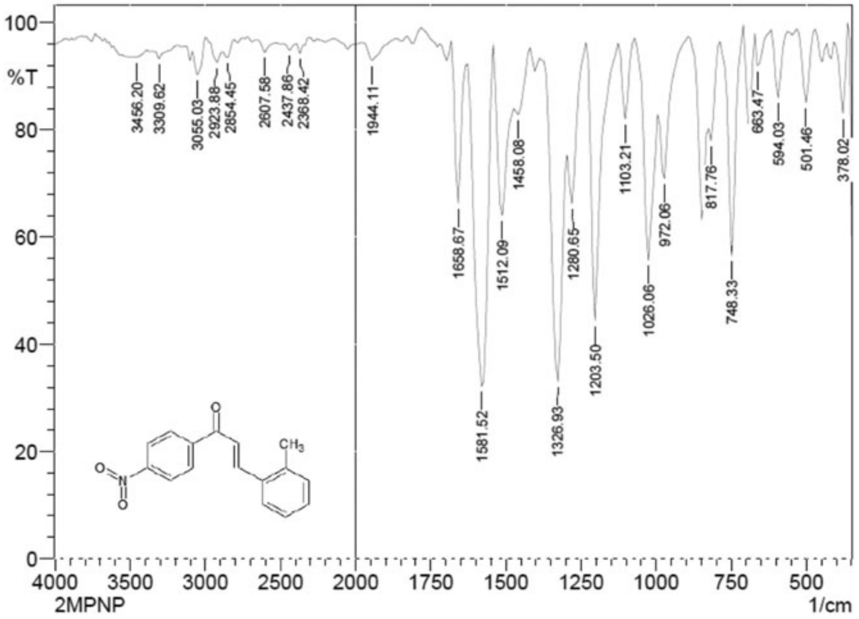

Figure 3. FTIR spectrum of 2MPNP.

Material Synthesis and Crystal Growth

(2*E*)-3-(2-methylphenyl)-1-(4-nitrophenyl)prop-2-en-1-one (2MPNP) was synthesized by Claisen–Schmidt condensation reaction as reported earlier [6, 17]. The starting materials used for the synthesis of 2MPNP are of Analytical Reagent (AR) grade chemicals procured from Sigma-Aldrich Company and were used without further purification. A solution of

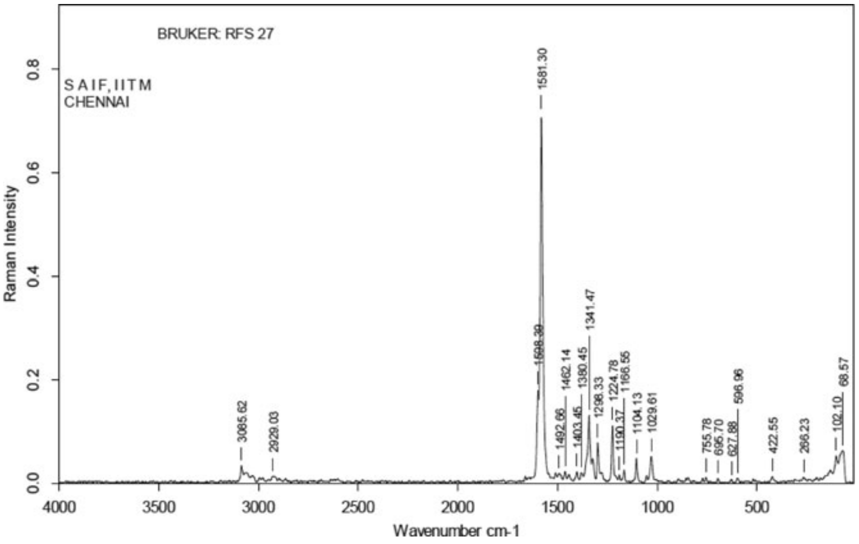

Figure 4. FT Raman spectrum of 2MPNP.

Table 1. Assignment of vibrational frequencies

Wave number (cm^{-1})		
Infrared lines	Raman lines	Assignment
3055.03	3085.62	Aromatic C—H Stretching
2923.88 and 2854.45	2929.03	Asymmetric and symmetric C—H stretching vibration of CH_3 group
1658.67	1598.39	C=O stretching vibration
1512.09	1492.66	C=C stretching vibration
1581.52 and 1326.93	1581.3 and 1341.47	Asymmetric and symmetric stretching vibration of NO_2 group
1458.08	1462.14	C—H bending vibrations of CH_3 group
1203.5	1298.33	C—H in plane deformation of CH=CH
1026–650	1029.61–755.78	C—H out of plane bending vibrations of hydrogen atom attached to unsaturated carbons

2-Methyl benzaldehyde (0.01 mol) and 4-nitroacetophenone (0.01 mol) in methanol (30 ml) were taken in a conical flask with stirring and kept at room temperature. Then, 20% sodium hydroxide (NaOH) solution (1 ml) was added gradually over a period of 10 min. The solution was stirred for another 30 min. The solution was then poured into the beaker

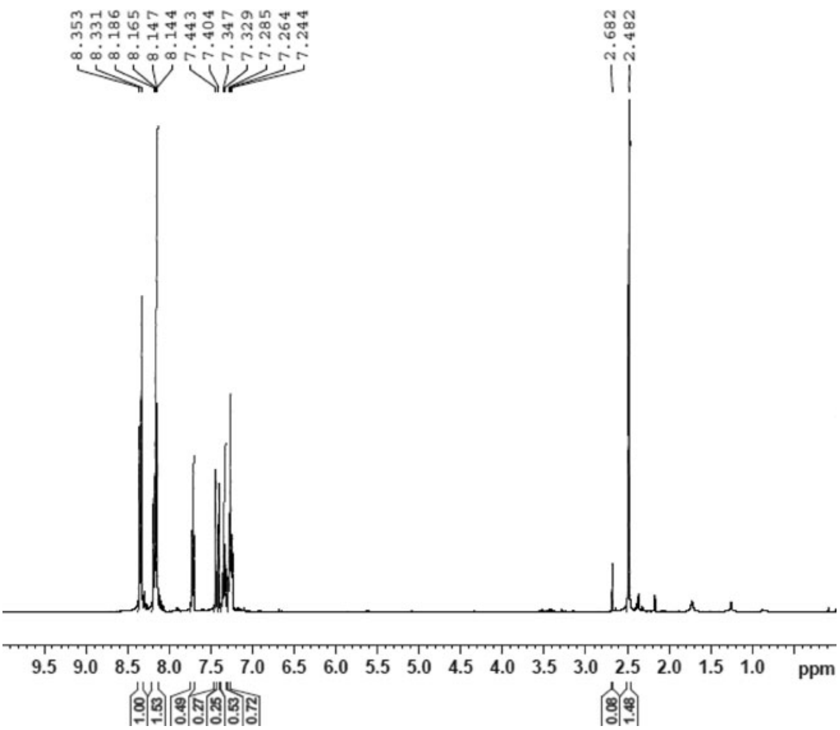

Figure 5a. NMR spectrum of 2MPNP.

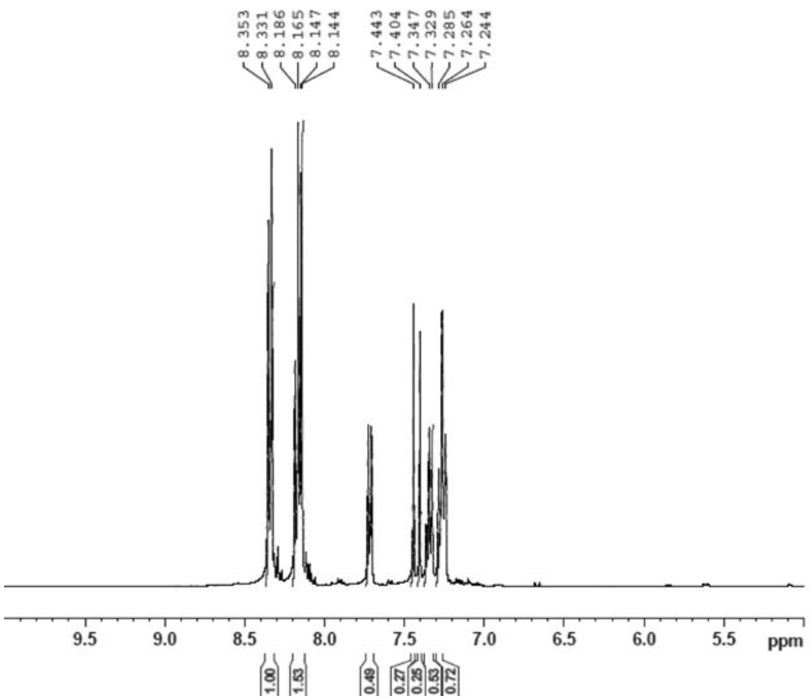

Figure 5b. NMR spectrum of 2MPNP.

containing ice-cold water and the separated crude product was filtered, washed with water and dried. Synthesized 2MPNP was purified by successive recrystallization from acetone. The synthetic scheme for the compound is given in Fig. 1.

The solubility of the compound was determined by adding the solvent to a known amount of 2MPNP till it completely dissolved. 2MPNP is expectedly insoluble in water, and moderately soluble in ethanol, methanol, acetone, and dimethyl formamide (DMF). Crystals were grown by the slow evaporation technique at room temperature [18] by using DMF as a solvent due to its moderate solubility and better control over the growth rate because of its slower evaporation rate. A saturated solution of 2MPNP in DMF was prepared, filtered, and kept in a dust free atmosphere. The tiny crystals nucleated during super saturation were allowed to grow in size and then harvested. Single-crystals are needle shaped and pale yellow in color and had the size of 11 × 1 × 1 mm^3 were grown in 10–15 days is shown in Fig. 2.

Characterization

FT-IR & Laser Raman Spectral Analysis

The Fourier transform infrared (FT-IR) and Laser Raman spectral analysis of 2MPNP was carried out to investigate the presence of functional groups and their vibrational modes. The sample used for FT-IR was prepared by mixing 2MPNP with KBr pellet. The FTIR spectrum was recorded between 400 and 4000 cm^{-1} using a SHIMADZU-8400S FT-IR spectrometer. FT-Raman spectrum of title compound was obtained using BRUKER RFS 27 FT-Raman spectrometer using an excitation wavelength of 1064 nm and 100 mW from

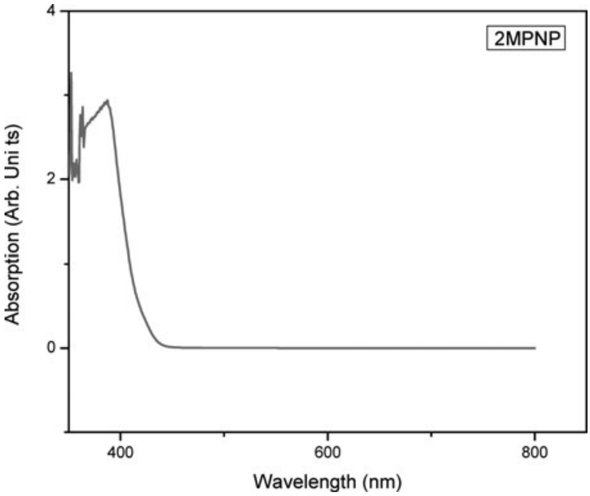

Figure 6. UV-Visible spectrum of 2MPNP.

Nd:YAG laser. The FT-IR and FT-Raman spectra of the compound are shown in Figs. 3 and 4 respectively.

In FT-IR spectrum, the weak intensity absorption band at 3055.03 cm^{-1} is due to the aromatic C—H stretch. The two weak absorption bands at 2923.88 cm^{-1} and 2854.45 cm^{-1} corresponds to the asymmetric and symmetric C—H stretching vibrations of CH_3 group. The conjugation of C=O with C=C increases its single bond character resulting in lower values of carbonyl stretching wavenumbers. The sharp intense band at 1658.67 cm^{-1} is assigned to C=O stretching mode. The intense band at 1512 cm^{-1} corresponds to C=C stretching vibration. The two very intense absorption bands at 1581.52 and 1326.93 cm^{-1} are due to asymmetric and symmetric stretching vibrations of NO_2 group. The less intense

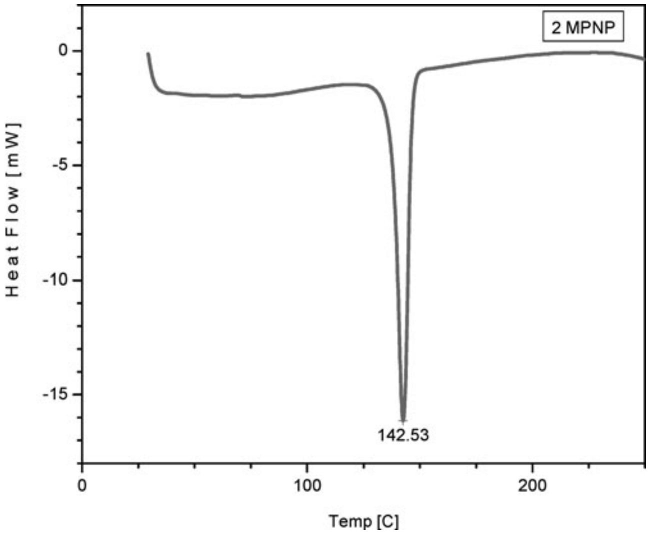

Figure 7. DSC curve of 2MPNP.

Table 2. SHG measurement results

Sample	Output signal amplitude in millivolts	SHG efficiency
Urea	101	
KDP	43	1.17 times Urea
2MPNP	118	2.75 times KDP

band at 1458.08 cm^{-1} corresponds to C—H bending vibrations of CH_3 group [19–22]. The characteristic FT-IR frequencies and the corresponding FT-Raman assignments are recorded in Table 1. The FT-IR and Raman spectra confirm the functional groups present in the 2MPNP.

NMR Spectroscopy

Nuclear Magnetic Resonance (NMR) spectrum was recorded for structural confirmation of 2MPNP. A small quantity of the sample was dissolved in the deuterated chloroform ($CDCl_3$) and ^{1}H NMR spectrum was recorded at 400 MHz using tetramethylsilane (TMS) as internal standard and is shown in Figs. 5a and b. The signals obtained in proton NMR spectra of the compound are in agreement with the structure of the title compound. The characteristic peaks observed in the spectrum are assigned as given below [19, 20].

^{1}H NMR ($CDCl_3$): δ: 2.482 (s, 3H of CH_3), 7.443–7.404 (d, 1H, —CH of —CH=CH—),7.329–7.285 (d, 1H, —CH of —CH=CH—), 8.353–8.331 (d, 2H, Ar–H of nitrophenyl ring), 8.186–8.165 (d, 2H, Ar–H of nitrophenyl ring), 8.144 (s, 1H, Ar–H of methyl phenyl ring), 7.285–7.244 (m, 3H Ar–H of methyl phenyl ring).

UV–Visible Spectrum

The UV–Visible absorption spectrum of the 2MPNP crystals dissolved in DMF was recorded using a SHIMADZU UV1601PC UV-Visible spectrophotometer in the wavelength range of 200–800 nm. A solution of 2MPNP in DMF was placed in a 1 cm thick

Table 3. Single crystal XRD data of 2MPNP [CCDC No. 946067]

Molecular formula	$C_{16}H_{13}NO_3$
Formula weight	267.27
Crystal color, habit	Pale yellow, needle
Crystal system	Orthorhombic
Space group	$Pca2_1$
Unit cell parameters	$a = 29.905(4)$Å $b = 4.8241(5)$ Å $c = 9.0984(10)$Å $\alpha = \beta = \gamma = 90.00$å $Z = 4.$
Cell volume	$v = 1312.58$ Å^3
Radiation used	MoK$_\alpha$ radiation of wavelength 0.71073 Å
Study temperature	295(2) K

Table 4. Bond lengths

Number	Atom1	Atom2	Length
1	O1	C7	1.222(5)
2	O2	N1	1.226(6)
3	O3	N1	1.210(6)
4	N1	C4	1.474(6)
5	C1	C2	1.391(5)
6	C1	C6	1.382(5)
7	C1	C7	1.498(5)
8	C2	H2	0.930(4)
9	C2	C3	1.380(6)
10	C3	H3	0.931(4)
11	C3	C4	1.374(6)
12	C4	C5	1.368(6)
13	C5	H5	0.929(4)
14	C5	C6	1.388(6)
15	C6	H6	0.930(4)
16	C7	C8	1.455(6)
17	C8	H8	0.929(4)
18	C8	C9	1.337(6)
19	C9	H9	0.931(4)
20	C9	C10	1.450(6)
21	C10	C11	1.396(6)
22	C10	C15	1.401(6)
23	C11	H11	0.931(4)
24	C11	C12	1.383(6)
25	C12	H12	0.929(5)
26	C12	C13	1.384(7)
27	C13	H13	0.930(5)
28	C13	C14	1.372(7)
29	C14	H14	0.931(5)
30	C14	C15	1.395(6)
31	C15	C16	1.505(6)
32	C16	H16A	0.960(5)
33	C16	H16B	0.959(5)
34	C16	H16C	0.960(5)

cuvette for measurement. The recorded spectrum is shown in Fig. 6. The crystal has a wider transparency range extending into the entire visible region with a lower cut off wavelength of 440 nm and hence is desirable for NLO applications at room temperature.

Thermal Analysis

The dimensional stability of compound with temperature is one of the important parameter for NLO materials. The thermal property of 2MPNP was studied in powder form by recording the differential scanning calorimeter (DSC) response curve in the temperature range

Table 5. Bond angles (°)

Number	Atom1	Atom2	Atom3	Angle
1	O2	N1	O3	123.8(5)
2	O2	N1	C4	118.2(4)
3	O3	N1	C4	118.0(4)
4	C2	C1	C6	118.8(3)
5	C2	C1	C7	117.7(3)
6	C6	C1	C7	123.6(3)
7	C1	C2	H2	119.3(4)
8	C1	C2	C3	121.4(4)
9	H2	C2	C3	119.3(4)
10	C2	C3	H3	120.8(4)
11	C2	C3	C4	118.3(4)
12	H3	C3	C4	120.9(4)
13	N1	C4	C3	118.0(4)
14	N1	C4	C5	120.0(4)
15	C3	C4	C5	122.0(4)
16	C4	C5	H5	120.4(4)
17	C4	C5	C6	119.3(4)
18	H5	C5	C6	120.3(4)
19	C1	C6	C5	120.3(4)
20	C1	C6	H6	119.9(4)
21	C5	C6	H6	119.8(4)
22	O1	C7	C1	118.1(4)
23	O1	C7	C8	121.3(4)
24	C1	C7	C8	120.6(3)
25	C7	C8	H8	119.4(4)
26	C7	C8	C9	121.2(4)
27	H8	C8	C9	119.4(4)
28	C8	C9	H9	115.5(4)
29	C8	C9	C10	129.0(4)
30	H9	C9	C10	115.5(4)
31	C9	C10	C11	120.5(4)
32	C9	C10	C15	120.7(4)
33	C11	C10	C15	118.8(4)
34	C10	C11	H11	119.5(4)
35	C10	C11	C12	121.2(4)
36	H11	C11	C12	119.4(4)
37	C11	C12	H12	120.1(5)
38	C11	C12	C13	119.9(4)
39	H12	C12	C13	120.0(5)
40	C12	C13	H13	120.3(5)
41	C12	C13	C14	119.5(4)
42	H13	C13	C14	120.2(5)
43	C13	C14	H14	119.1(5)
44	C13	C14	C15	121.8(4)

(Continued on next page)

Table 5. Bond angles (°) *(Continued)*

Number	Atom1	Atom2	Atom3	Angle
45	H14	C14	C15	119.1(4)
46	C10	C15	C14	118.9(4)
47	C10	C15	C16	121.9(4)
48	C14	C15	C16	119.2(4)
49	C15	C16	H16A	109.5(4)
50	C15	C16	H16B	109.5(4)
51	C15	C16	H16C	109.5(4)
52	H16A	C16	H16B	109.5(5)
53	H16A	C16	H16C	109.4(5)
54	H16B	C16	H16C	109.5(5)

30°C to 250°C, at a rate of 10°C/min, in nitrogen atmosphere using SHIMADZU Differential Scanning Calorimeter (DSC-60). The DSC plot is shown in Fig. 7. The endothermic peak shown at 142.53°C, corresponds to the melting point of title compound indicating that the compound can be used up to a significantly higher temperatures without affecting crystal stability.

NLO Property

The relative SHG efficiency of the grown crystal was measured by the Kurtz and Perry powder technique [23]. For this study, a powdered sample of 2MPNP was taken in a capillary tube. A fundamental beam of wavelength 1064 nm, energy 2.3 mJ/pulse, pulse width 10 ns and at an input rate of 10 Hz from a Q-switched Nd:YAG laser was passed through the sample. A photomultiplier tube (Hamamatsu-R 2059) detects the second harmonic wave of wavelength 532 nm generated from the sample and was converted into electrical signal. The converted electrical signal was displayed on an oscilloscope (Tektronix-TDS 3052B). The signal amplitude in volts is compared with that of standard urea and potassium dihydrogen phosphate (KDP) crystals powdered into identical size.

The SHG efficiency of the 2MPNP was found to be 1.17 times that of urea and 2.75 times that of KDP. The results are shown in Table 2.

Single Crystal X-Ray Diffraction Studies

A single crystal X-ray diffraction (XRD) study of 2MPNP was carried out using Bruker SMART APEX diffractometer. The structure was solved using SHELXS-97 and refined using SHELXL-97 [24]. A good quality single crystal of dimension 0.4 × 0.4 × 0.4 mm^3 was selected under a polarizing microscope and used for data collection. The data was collected at 295 K using Mo K_α radiation. From single crystal XRD studies it has been found that 2MPNP crystallizes in the orthorhombic crystal class in the noncentrosymmetric space group $Pca2_1$. The molecule of the title compound exists in most stable *E*-configuration with respect to the C7=C8 double bond. The molecule has a dihedral angle between the 4-nitrobenzene and 2-methylphenyl rings of 9.15°. The crystallographic details are provided in Table 3. Tables 4–6 gives the list of bond lengths, bond angles and torsion angles respectively.

Table 6. Torsion angles

Atom1	Atom2	Atom3	Atom4	Torsion
O2	N1	C4	C3	4.6(6)
O2	N1	C4	C5	−174.7(4)
O3	N1	C4	C3	−175.5(4)
O3	N1	C4	C5	5.2(6)
C6	C1	C2	H2	179.6(4)
C6	C1	C2	C3	−0.3(6)
C7	C1	C2	H2	−1.2(6)
C7	C1	C2	C3	178.9(4)
C2	C1	C6	C5	0.5(6)
C2	C1	C6	H6	−179.4(4)
C7	C1	C6	C5	−178.6(4)
C7	C1	C6	H6	1.4(7)
C2	C1	C7	O1	−6.7(6)
C2	C1	C7	C8	175.1(4)
C6	C1	C7	O1	172.5(4)
C6	C1	C7	C8	−5.7(6)
C1	C2	C3	H3	179.9(4)
C1	C2	C3	C4	−0.1(6)
H2	C2	C3	H3	−0.1(7)
H2	C2	C3	C4	179.9(4)
C2	C3	C4	N1	−178.8(4)
C2	C3	C4	C5	0.5(6)
H3	C3	C4	N1	1.2(7)
H3	C3	C4	C5	−179.5(4)
N1	C4	C5	H5	−1.0(7)
N1	C4	C5	C6	179.0(4)
C3	C4	C5	H5	179.7(4)
C3	C4	C5	C6	−0.3(7)
C4	C5	C6	C1	−0.2(6)
C4	C5	C6	H6	179.8(4)
H5	C5	C6	C1	179.8(4)
H5	C5	C6	H6	−0.3(7)
O1	C7	C8	H8	179.9(4)
O1	C7	C8	C9	−0.1(6)
C1	C7	C8	H8	−1.9(6)
C1	C7	C8	C9	178.0(4)
C7	C8	C9	H9	−0.7(6)
C7	C8	C9	C10	179.2(4)
H8	C8	C9	H9	179.2(4)
H8	C8	C9	C10	−0.9(7)
C8	C9	C10	C11	−2.4(7)
C8	C9	C10	C15	179.1(4)
H9	C9	C10	C11	177.6(4)
H9	C9	C10	C15	−1.0(6)

(Continued on next page)

Table 6. Torsion angles *(Continued)*

Atom1	Atom2	Atom3	Atom4	Torsion
C9	C10	C11	H11	−0.5(7)
C9	C10	C11	C12	179.6(4)
C15	C10	C11	H11	178.1(4)
C15	C10	C11	C12	−1.8(6)
C9	C10	C15	C14	−179.5(4)
C9	C10	C15	C16	0.3(6)
C11	C10	C15	C14	1.9(6)
C11	C10	C15	C16	−178.3(4)
C10	C11	C12	H12	−178.6(4)
C10	C11	C12	C13	1.4(7)
H11	C11	C12	H12	1.5(8)
H11	C11	C12	C13	−178.5(5)
C11	C12	C13	H13	178.9(5)
C11	C12	C13	C14	−1.1(7)
H12	C12	C13	H13	−1.2(8)
H12	C12	C13	C14	178.8(5)
C12	C13	C14	H14	−178.8(5)
C12	C13	C14	C15	1.3(7)
H13	C13	C14	H14	1.2(8)
H13	C13	C14	C15	−178.7(5)
C13	C14	C15	C10	−1.7(7)
C13	C14	C15	C16	178.5(4)
H14	C14	C15	C10	178.4(4)
H14	C14	C15	C16	−1.4(7)
C10	C15	C16	H16A	176.6(4)
C10	C15	C16	H16B	56.6(6)
C10	C15	C16	H16C	−63.5(6)
C14	C15	C16	H16A	−3.6(6)
C14	C15	C16	H16B	−123.6(5)
C14	C15	C16	H16C	116.3(5)

An ORTEP plot of the 2MPNP molecule is shown in Fig. 8 with 50% ellipsoidal probability and H atoms are shown as small spheres of arbitrary radii. The crystal packing diagram of molecule depicting C—H···O intermolecular hydrogen bond viewed down along crystallographic *a*, *b*, and *c* axis are shown in Fig. 9–11.

Structure-NLO Property Relationship

The 2MPNP molecule contains an electron donor methyl group attached to the ortho position of one of the benzene ring and an electron acceptor nitro group attached to the para position of the other benzene ring. The two rings are connected through a π-conjugated system with a carbonyl group (—C=O—), thus forming D–π–A type structure. The charge transfer takes place through the π-conjugation pathway formed by carbon-carbon double bond connecting

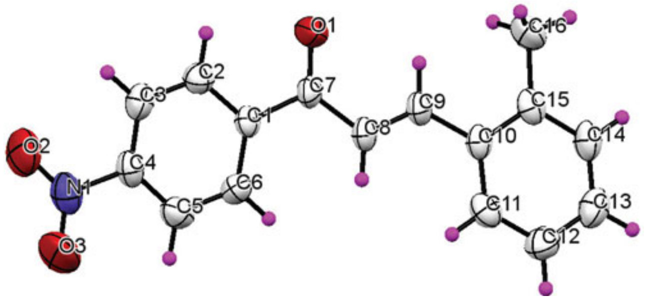

Figure 8. ORTEP of 2MPNP molecule with 50% ellipsoidal probability and H atoms are shown as small spheres of arbitrary radii.

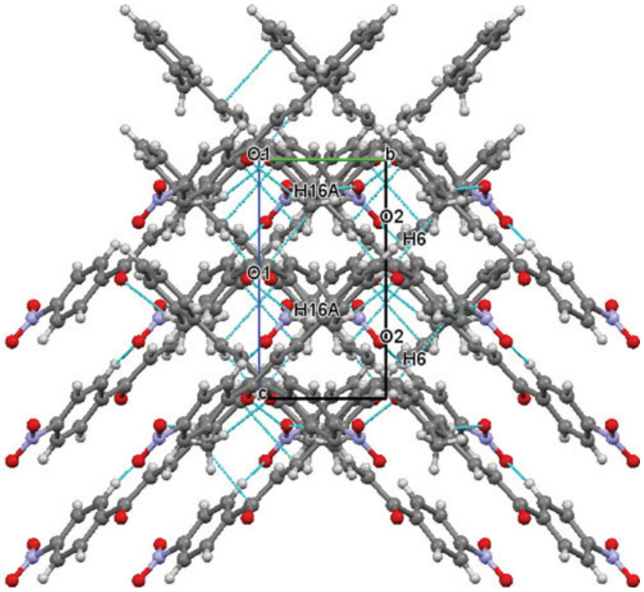

Figure 9. Crystal packing diagram of molecule viewed down along crystallographic a-axis.

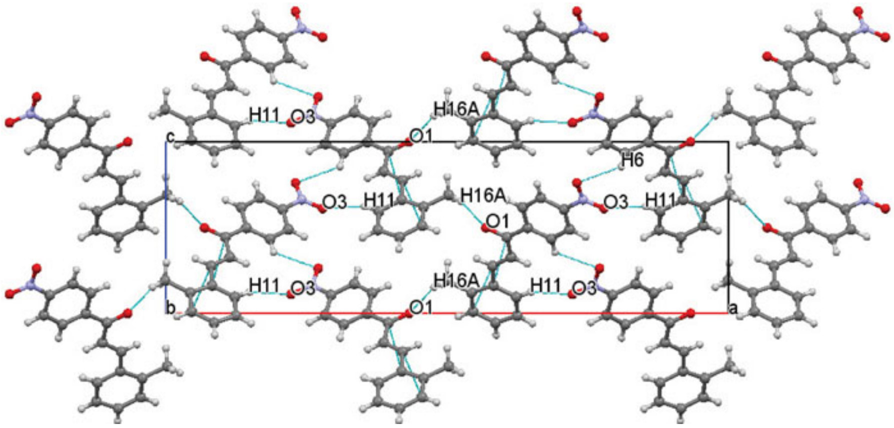

Figure 10. Crystal packing diagram of molecule viewed down along crystallographic b-axis.

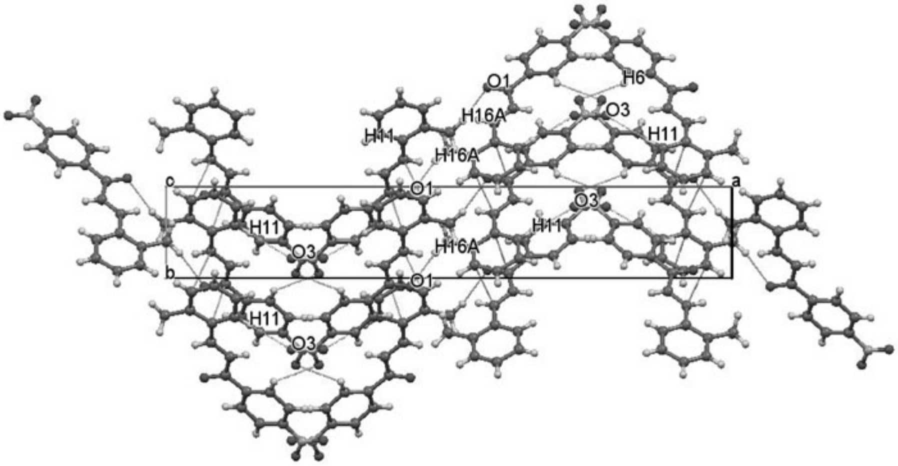

Figure 11. Packing diagram of molecule depicting C—H···O intermolecular hydrogen bond viewed down along crystallographic "c" axis.

the electron donor and acceptor groups. This ensures the electronic delocalization within the molecule which helps to possess optical nonlinearity.

Conclusion

A novel organic NLO material 2MPNP has been synthesized and single crystal was prepared. The formation of compound was confirmed by FT-IR NMR spectral studies. Single-crystal XRD study reveals the crystal structure belongs to orthorhombic crystal class in the non-centrosymmetric space group $Pca2_{1.}$ This crystal has SHG efficiency of 1.17 times that of urea and 2.75 times that of KDP. The good transparency, thermal stability and high SHG efficiency shows that the crystals can be used for frequency doubling and other NLO applications.

Acknowledgments

Authors are thankful to the University of Malaya for the crystal structure determination of 2MPNP and DST-SAIF, IIT Madras, Chennai for FT-Raman facility.

References

[1] Chemla, D. S., & Zyss, J. (1987). *Nonlinear Optical Properties of Organic Molecules and Crystals*, Academic Press: New York.

[2] Prasad, P. N., & Williams, D. J. (1991). *Introduction to Nonlinear Optical Effects in Organic Molecules and Polymers*, Wiley: New York.

[3] Hann, R. A., & Bloor, D. (1989). *Organic Materials for Non-linear Optics*, The Royal Society of Chemistry: London.

[4] Prasad, P. N., & Ulrich, D. R. (1988). *Non-Linear Optical and Electroactive Polymers*, Plenum: New York.

[5] Nalwa, H. S., & Miyata, S. (1997). *Nonlinear Optics of Organic Molecules and Polymers*, CRC Press: New York.

[6] Dhar, D. N., (1981). *The Chemistry of Chalcones and Related Compounds*, Wiley: New York.

[7] Uchida, T., Kozawa, K., Sakai, T., Aoki, M., Yoguchi, H., *et al.* (1998). *Mol. Cryst. Liq. Cryst.*, *315*, 135.

[8] Ravindra, H. J., Kiran, A. J., Satheesh, R. N., Dharmaprakash, S. M., Chandrasekharan, K. *et al.* (2008). *J. Crystal Growth*, *310*, 2543.

[9] Kiran, A. J., Kim, H. C., Kim, K., Rotermund, F., Ravindra, H. J., *et al.* (2008). *Appl. Phys. Lett.*, *92*, 113307.

[10] Reinhardt, B. A., Brott, L. L., Clarson, S. J., Dillard, A. G., Bhatt, J. C., *et al.* (1998). *Chem. Mater.*, *10*, 1863.

[11] Albota, M., Beljonne, D., Bredas, J. L., Ehrlich, J. E., Fu, J. Y., *et al.* (1998). *Science*, *281*, 1653.

[12] Shubhalaxmi, Hahne, S., Jayarama, A., & Subrahmanya Bhat, K. (2013). *Chem. Sci. Trans.*, *2*(3), 829.

[13] Shubhalaxmi, Hahne, S., Zischille, C., Jayarama, A., & Subrahmanya Bhat, K. (2013). *Chem. Sci. Trans.*, *2*(3), 841.

[14] Prabhu, A. N., Jayarama, A., Subrahmanya Bhat, K., and Upadhyaya, V. (2013). *J. Molecular Struct.*, *1031*, 79.

[15] Prabhu, A. N., Jayarama, A., Upadhyaya, V., & Subrahmanya Bhat, K. (2013). *Mat. Chem. Phy.*, *138*, 179.

[16] Prabhu, A. N., Jayarama, A., Subrahmanya Bhat, K., Manjunatha, K. B., Umesh, G., *et al.* (2013). *Ind. J. Mat. Sci.*, *5*, Article ID 151230.

[17] Vogel, A. I., & Furniss, B. S. (1999). *Vogel's Textbook of Practical Organic Chemistry*, 5th ed., Longman Group: London.

[18] Brice, J. C. (1973). *Crystal Growth from Solution*, North-Holland: Amsterdam.

[19] Pavia, D. L., Gary, M. L., & George, S. K. (2001). *Introduction to Spectroscopy*, 3rd ed., Thomson Learning: US.

[20] Kalsi, P. S. (1995). *Spectroscopy of Organic Compounds*, 2nd ed, Wiley Eastern Limited: New Delhi.

[21] Ravindra, H. J., Kiran, A. J., Satheesh, R. N., Dharmaprakash, S. M., Chandrasekharan, K., *et al.* (2008). *J. Crystal Growth*, *310*, 4169.

[22] Abraham, J. P., Sajan, D., Venkatraya S., Dharmaprakash, S. M., Nemec, I., *et al.* (2009). *J. Molecular Structure*, *917*, 27.

[23] Kurtz, S. K., & Perry, T. T. (1968). *J. Appl. Phys.*, *39*, 3798.

[24] Sheldrick, G. M. (2008). *Acta Cryst.*, *A 64*, 112.